Cerebral Cortex, 2018; 1–13

doi: 10.1093/cercor/bhy174
Original Article

ORIGINAL ARTICLE

Hippocampal Network Oscillations Rescue Memory Consolidation Deficits Caused by Sleep Loss

Nicolette Ognjanovski[1], Christopher Broussard[2], Michal Zochowski[3,4] and Sara J. Aton[1]

[1]Department of Molecular, Cellular, and Developmental Biology, University of Michigan, Ann Arbor, MI 48109, USA, [2]Information Technology Advocacy and Research Support, College of Literature, Science, and the Arts, University of Michigan, Ann Arbor, MI 48109, USA, [3]Program in Biophysics, University of Michigan, Ann Arbor, MI 48109, USA and [4]Department of Physics, University of Michigan, Ann Arbor, MI 48109, USA

Address correspondence to Sara J. Aton, Department of Molecular, Cellular, and Developmental Biology, University of Michigan, 4268 Biological Sciences Building, 1105 N. University Ave., Ann Arbor, MI 48109, USA. Email: saton@umich.edu

Abstract

Oscillations in the hippocampal network during sleep are proposed to play a role in memory storage by patterning neuronal ensemble activity. Here we show that following single-trial fear learning, sleep deprivation (which impairs memory consolidation) disrupts coherent firing rhythms in hippocampal area CA1. State-targeted optogenetic inhibition of CA1 parvalbumin-expressing (PV+) interneurons during postlearning NREM sleep, but not REM sleep or wake, disrupts contextual fear memory (CFM) consolidation in a manner similar to sleep deprivation. NREM-targeted inhibition disrupts CA1 network oscillations which predict successful memory storage. Rhythmic optogenetic activation of PV+ interneurons following learning generates CA1 oscillations with coherent principal neuron firing. This patterning of CA1 activity rescues CFM consolidation in sleep-deprived mice. Critically, behavioral and optogenetic manipulations that disrupt CFM also disrupt learning-induced stabilization of CA1 ensembles' communication patterns in the hours following learning. Conversely, manipulations that promote CFM also promote long-term stability of CA1 communication patterns. We conclude that sleep promotes memory consolidation by generating coherent rhythms of CA1 network activity, which provide consistent communication patterns within neuronal ensembles. Most importantly, we show that this rhythmic patterning of activity is sufficient to promote long-term memory storage in the absence of sleep.

Key words: hippocampus, memory consolidation, network oscillations, sleep

Introduction

Sleep affects many aspects of brain physiology, including neuronal activity, neurotransmission, neuromodulation, transcription, and translation (Puentes-Mestril and Aton 2017). While sleep can promote cognitive processes such as long-term memory formation, the precise mechanism by which it does so is unknown. A long-standing hypothesis is that the oscillations in network activity that are characteristic of sleep states play an essential role in memory storage (Diekelmann and Born 2010; Aton 2013; Inostroza and Born 2013). A significant body of recent evidence has led to the hypothesis that offline "reactivation" of specific populations of hippocampal neurons, coordinated by network oscillations, could drive long-term memory formation (Kudrimoti et al. 1999; Dupret et al. 2010; Carr et al.

2012; Ognjanovski et al. 2017). Current data suggest that consolidation of episodic and spatial memories may be promoted by hippocampal network oscillations occurring in NREM and REM sleep. Such network oscillations could play a role in patterning activity in neuronal ensembles (Kudrimoti et al. 1999; Csicsvari et al. 1999b; Itskov et al. 2008; Ognjanovski et al. 2017).

We have previously shown that in mice, CFM consolidation is associated with augmented CA1 network oscillations during post-contextual fear conditioning (CFC) REM and NREM sleep (Ognjanovski et al. 2014). These oscillations—including NREM delta (a.k.a., "slow wave"; 0.5–4 Hz), REM theta (4–12 Hz), and sharp-wave ripple oscillations (SPWRs; 150–200 Hz)—are augmented by the activity of CA1 PV+ interneurons in the hours following CFC (Ognjanovski et al. 2017; Xia et al. 2017). Circuit-level manipulations aimed at disrupting CA1 delta, theta, or SPWR oscillations (or thalamocortical sleep spindles; 7–15 Hz) through various means have been shown to interfere with memory consolidation (Girardeau et al. 2009; Mednick et al. 2013; Boyce et al. 2016; Ognjanovski et al. 2017; Xia et al. 2017). These data support the hypothesis that network oscillations are an essential element for sleep-dependent cognitive functions (Diekelmann and Born 2010; Tononi and Cirelli 2014; Crunelli et al. 2018). For example, recent data have shown that augmenting thalamocortical network oscillations, in human subjects, during sleep can promote memory consolidation (Mednick et al. 2013; Ngo et al. 2013; Westerberg et al. 2015; Ong et al. 2016). However, it is unclear whether sleep-associated network oscillations are sufficient to promote memory storage (in any circuit) in the absence of sleep. The present study, focused on hippocampally generated oscillations, is the first experimental test addressing this question.

Despite extensive evidence that such network oscillations pattern neuronal activity, both within the hippocampus (Csicsvari et al. 1999b; Dragoi and Buzsaki 2006; Carr et al. 2012; Ognjanovski et al. 2017; Xia et al. 2017), and between the hippocampus and other structures (Ribeiro et al. 2004; Wierzynski et al. 2009; Latchoumane et al. 2017; Rothschild et al. 2017; Xia et al. 2017), how such patterning promotes long-term memory storage remains unknown. A great deal of recent work has focused on the potential role of sequential "replay" of activity patterns occurring during prior experience (Puentes-Mestril and Aton 2017). Available data suggests that manipulations of pattern replay occurring immediately after learning disrupt memory storage (Girardeau et al. 2009). However, many forms of memory consolidation remain susceptible to disruption of network activity for hours or even days following a learning event (Knowlton et al. 1985; Daumas et al. 2005; Ross and Eichenbaum 2006; Goshen et al. 2011)—that is, long after sequential replay (which occurs over a period of several minutes following experience) has come to an end. Further, because sequential replay is typically seen after extensive training on a task, it remains unclear whether it plays a causal role in promoting memory formation, or is the result of activity propagating through well-established circuits (Puentes-Mestril and Aton 2017). Our prior work has suggested that another feature of postlearning CA1 network behavior, stabilization of functional communication patterns between neurons (over a timescale of several hours), could be a better correlate of de novo memory storage (Ognjanovski et al. 2014, 2017). However, the relationship of sleep and sleep-associated oscillations to this network behavior is unknown. To address these questions, we have recorded neuronal and network activity from CA1 during CFM consolidation, with or without manipulations of behavioral state (i.e., sleep deprivation [SD]) or network activity (i.e., state-targeted optogenetic manipulations).

Materials and Methods

Mouse Handling and Surgical Procedures

All animal husbandry and surgical/experimental procedures were approved by the University of Michigan Institutional Animal Care and Use Committee. With the exception of fear conditioning and fear memory testing, mice were individually housed in standard caging with beneficial environmental enrichment (nesting material, treats and manipulanda) throughout all postoperative procedures. Lights were maintained on a 12 h:12 h light:dark cycle (lights on at 8 AM), and food and water were provided ad lib. At age 2–5 months, C57BL/6J mice (n = 10; IMSR_JAX:000 664, Jackson) were implanted with custom-built, driveable head stages with 2 bundles of stereotrodes for single unit/local field potential (LFP) recording, and nuchal muscle wires for electromyographic (EMG) recording, as previously described (Ognjanovski et al. 2014,

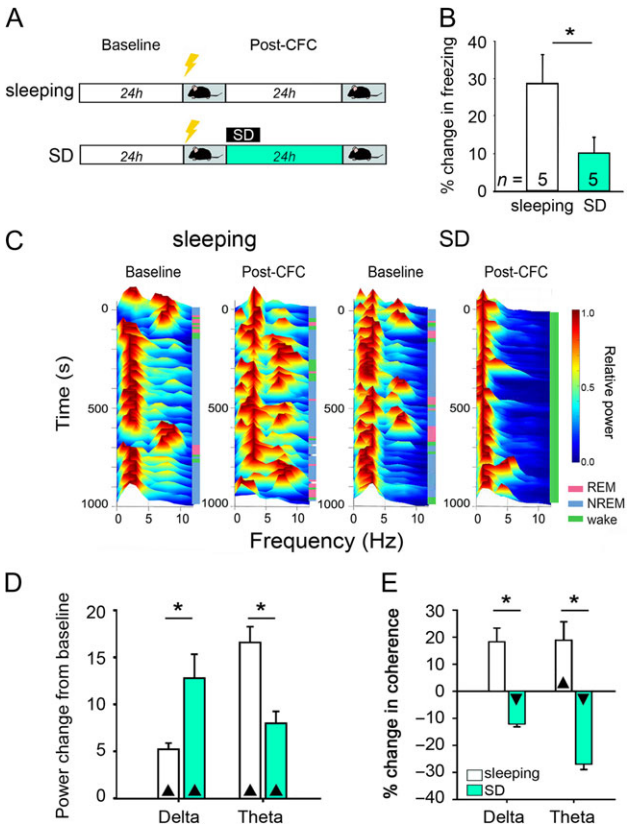

Figure 1. Post-CFC sleep is necessary for memory consolidation, alterations in CA1 neuronal firing, and enhanced CA1 network oscillations. (*A*) Experimental paradigm. Following a 24-h baseline recording period, all mice underwent single-trial CFC, after which they were returned to their home cage for either *ad lib* sleep (sleeping) or 6 h of sleep deprivation followed by recovery sleep (SD). (*B*) Context-specific freezing was reduced in SD mice 24 h after CFC. *$P < 0.05$, Student's t-test. n Indicates the number of mice per group. (*C*) Representative min–max normalized spectrograms of CA1 LFP recordings, showing relative increases in theta activity in the first 6 h following CFC in freely sleeping mice, which were suppressed in SD mice. (*D*) While CA1 LFP delta power was increased in SD mice relative to sleeping mice over the first 6 h post-CFC, SD reduced LFP theta activity. n = 5 and 5 CA1 recordings for sleeping and SD groups, respectively. *$P < 0.001$ for sleeping versus SD, ▲$P < 0.05$ for all baseline versus post-CFC comparisons, Holm–Sidak post hoc test. (*E*) In freely sleeping mice, CA1 neurons' firing coherence at delta and theta frequency bands increased over the first 6 h post-CFC. This increase was blocked by SD. n = 50 and 39 stably recorded neurons for sleeping and SD groups, respectively.*$P = 0.008$ for sleeping versus SD, ▲$P < 0.01$ and ▼$P < 0.001$ for baseline versus post-CFC comparisons, Holm–Sidak post hoc test. All bar graphs indicate mean ± SEM values for each group.

2017). The 2 stereotrode bundles were spaced approximately 1.0 mm apart within right hemisphere CA1 (relative to Bregma: 1.75–2.75 mm posterior, 1.5–2.5 mm lateral, and 1.0 mm ventral). CA1 recording sites for these experiments are shown in Supplementary Material, Fig. S1A. Behavioral and electrophysiological data from one group of C57BL/6J mice (CFC + *ad lib* sleep) were reported in a previous publication (Ognjanovski et al. 2017).

Two groups of mice were used to assess the effects of optogenetic manipulation of PV+ interneurons. For experiments shown in Figures 2–7, *Pvalb-IRES-CRE* mice ([B6;129P2-Pvalb$^{tm1(cre)Arbr}$/J; IMSR_JAX:008 069, Jackson] were crossed to either *B6.Cg-Gt(ROSA)26Sor*$^{tm40.1(CAG-aop3/EGFP)Hze}$*/J*, B6;129S-Gt[ROSA]*26Sor*$^{tm32(CAG-COP4*H134R/EYFP)Hze}$*/J*, or *B6.Cg-Gt(ROSA)26Sor*$^{tm6(CAG-ZsGreen1)Hze}$*/J* transgenic mice [RRID:IMSR_JAX:021 188, IMSR_JAX:012 569, and IMSR_JAX:007 906, Jackson]). This led to expression of either Arch (*PV::Arch*), ChR2 (*PV::ChR2*) or eGFP (*PV::GFP*), respectively, in PV+ interneurons. At age 2–5 months, male *PV::Arch* (n = 14), *PV::ChR2* (n = 7), and *PV::GFP* (n = 13) mice were implanted with custom-built, driveable head stages as described above. The 2 stereotrode bundles were spaced approximately 4.0 mm apart with one bundle each in right and left hemisphere CA1 (relative to Bregma: 1.75–2.75 mm posterior, 1.5–2.5 mm lateral, and 1.0 mm ventral). An optical fiber was placed adjacent to each bundle (i.e., in both hemispheres) in the recording array for delivery of laser light. To prevent light scatter during optogenetic procedures, implants were coated in black paint, and optical fibers and connectors were covered in black heat-shrink tubing. CA1 recording sites for these experiments are shown in Supplementary Material, Figures S4 and S7A.

Recording procedures

Mice were prepared for chronic stereotrode recording 1 week after implantation surgery as previously described. Briefly, mice were gently handled over a period of 5 days, for at least 10 min/day. During this time, electrode bundles were lowered into the hippocampus in 30 µm steps until stable recordings were achieved, with the same waveforms continuously present on recording channels for at least 24 h. After obtaining stable neuronal recordings, a continuous 24-h baseline recording period began at lights-on (ZT0). To characterize changes in neuronal and network activity associated with consolidation of CFM, recordings continued through subsequent single-trial CFC and the 24-h period between CFC and CFM testing. Neuronal spike and LFP signals were acquired by differentially filtering data from each electrode wire (bandpass 300 Hz–8 kHz and 0.5–300 Hz, respectively); these data were digitized and amplified using Plexon Omniplex hardware and software. Individual neurons were tracked throughout the experiment as described previously (see below) (Ognjanovski et al. 2014, 2017).

Contextual Fear Conditioning and Sleep Deprivation

Following 24-h baseline recording (and within 1 h of lights-on; ZT0–1), mice underwent single-trial CFC (Ognjanovski et al. 2014). Briefly, mice were placed in a novel Plexiglas chamber with a grid floor and allowed to explore for 2.5 min, after which they received a 2-s, 0.75 mA foot shock. Following foot shock, mice remained in the chamber for an additional 28 s. After CFC, all mice were returned to their home cage, and either were allowed *ad lib* sleep (with or without optogenetic manipulations), or were sleep deprived for the first 6 h following training (a manipulation which is sufficient to disrupt contextual fear memory [CFM] consolidation; SD). Gentle handling procedures used for SD were as described previously (Aton et al. 2014;

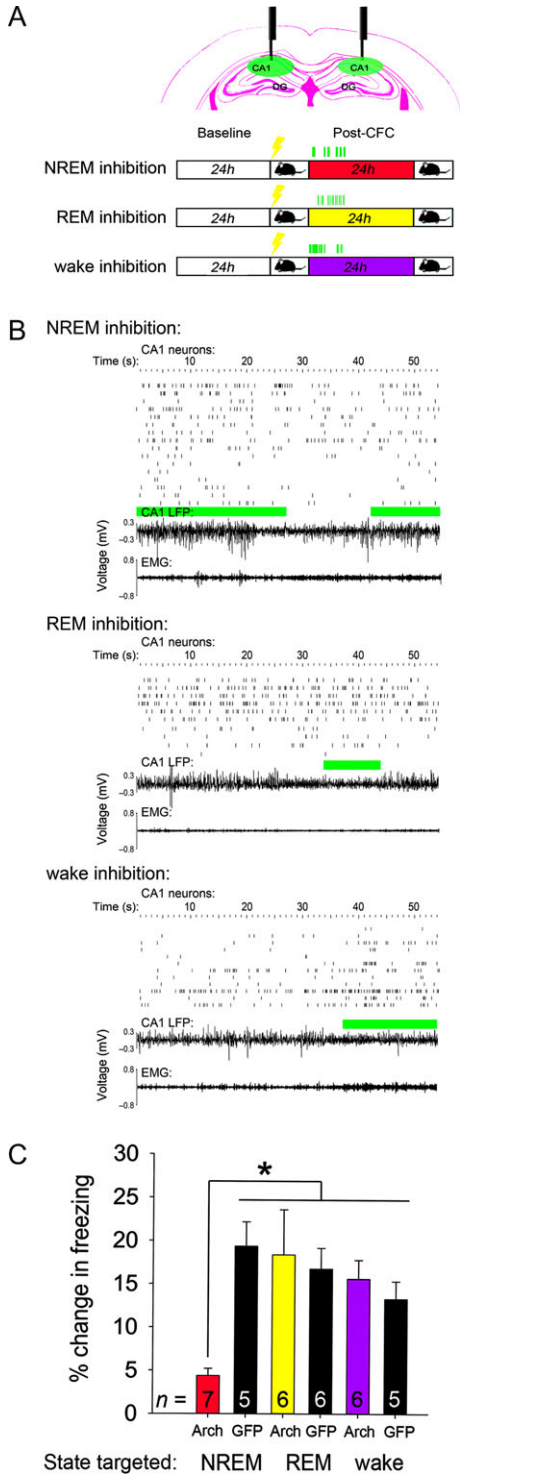

Figure 2. PV+ interneuron activity is critical during NREM sleep for CFM consolidation. (*A*) *Top*—coronal view showing relative placement of electrodes and optical fibers in CA1, with *PV::GFP* labeled neurons. *Bottom*—Experimental paradigm, indicating state-targeted 532 nm light delivery to CA1 over the first 6 h of post-CFC sleep. Procedures were identical for *PV::Arch* and *PV::GFP* mice. (*B*) Example traces of CA1 neurons' spike rasters, LFP activity, and EMG signals from representative *PV::Arch* mice in NREM inhibition, REM inhibition, and wake inhibition groups. Green bars indicate periods during which light was delivered to CA1 bilaterally. (*C*) Context-specific freezing was quantified 24 h following CFC for all treatment groups. CFM was impaired following NREM-targeted inhibition of PV+ interneurons, but not disrupted by inhibition targeted to REM or wake. *P = 0.008, Holm–Sidak post hoc test. n Indicates the number of mice per group.

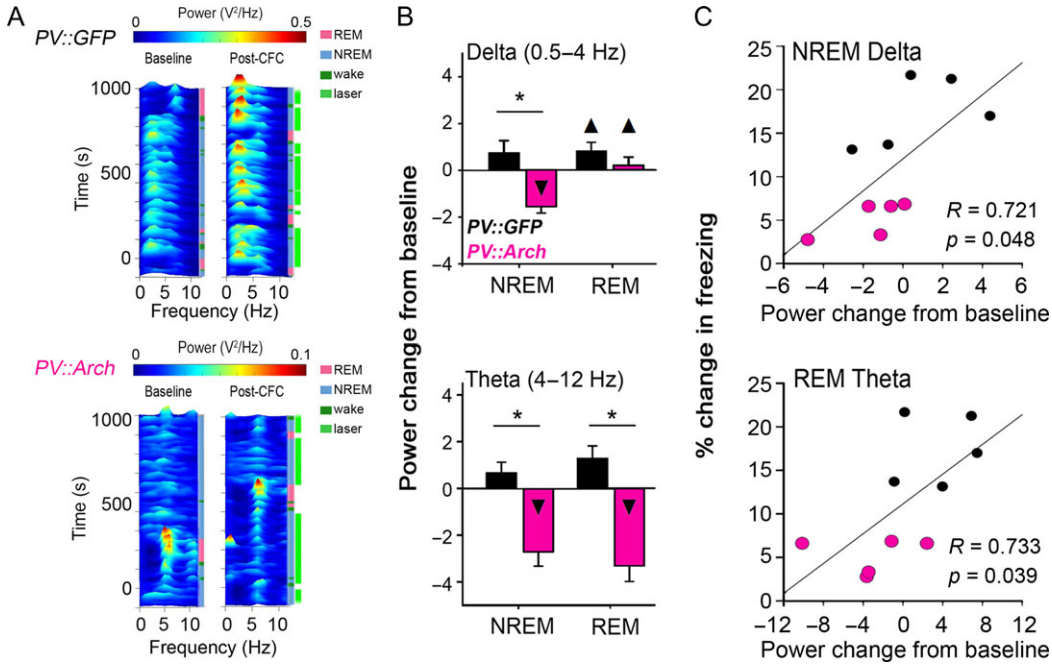

Figure 3. NREM-targeted PV+ interneuron inhibition disrupts CA1 network oscillations associated with CFM consolidation. (*A*) Representative CA1 LFP spectrograms, showing raw spectral power for recording intervals during the first 6 h of baseline and post-CFC periods. A 532 nm light was delivered to CA1 bilaterally during the intervals indicated in bright green at the far right of post-CFC spectrograms, targeted to intervals of NREM. (*B*) Inhibition of PV+ interneurons during NREM sleep significantly reduced NREM delta and theta power, and also affected REM theta power, in the first 6 h post-CFC. *$P < 0.001$ for *PV::GFP* versus *PV::Arch*, ▲$P < 0.05$ and ▼$P < 0.001$ for baseline versus post-CFC, Holm–Sidak post hoc test; $n = 8$ and 8 CA1 recordings for *PV::GFP* and *PV::Arch* groups, respectively. All bar graphs indicate mean ± SEM values for each group. (*C*) Post-CFC changes in NREM delta and in REM theta predicted the success of CFM consolidation for individual animals. *R* and Bonferroni-corrected *P* values indicate results of Spearman rank order.

Durkin et al. 2017), under normal room light, and included cage tapping, light touch with a cotton-tipped applicator, and (if necessary) disturbance of nesting material. These interventions were carried out as needed, and only when mice nested and assumed a stereotypic sleep posture. Mice were never directly handled during SD. For all SD experiments, mice were awake for >85% of the 6-h SD period on average (see Supplementary Material, Figs S1B and S7B). All mice were allowed *ad lib* sleep for the remainder of the recording (e.g., after SD). And 24 h following training, mice were returned to the conditioning chamber for 5 min to assess CFM. CFM was measured quantitatively as the change in context-specific freezing behavior between testing and training trials (i.e., % time spent freezing at test – % time spent freezing at baseline [preshock]). Post hoc scoring of videos for each CFC and CFM test trial was carried out by an observer blind to treatment. Freezing behavior was defined (and discriminated from quiet wake) by crouched, rigid posture with an absence of all body movement save respiration (including an absence of head and whisker movement).

State-Targeted Optogenetic Inhibition and Optogenetic Stimulation of PV+ Interneurons

For the experiments shown in Figures 2–3, *PV::Arch* and *PV::GFP* transgenic mice underwent state-targeted light delivery to dorsal CA1 across the first 6 h following CFC (from ZT 0–1 to ZT 6–7). Following baseline recording, mice were randomized into treatment groups, and subsequently received bilateral, 532 nm laser light delivery (Laserglow) for inhibition of PV+ CA1 interneurons during bouts of either NREM, REM, or wake. Light output at the fiber tip was estimated at 3 mW for all recordings during optogenetic inhibition. For state targeting, data from LFPs, EMGs, and live video recording were used to determine the animal's state in real time. After this 6-h period of inhibition, mice were allowed *ad lib* sleep for the next 18 h until CFM testing. Post hoc analysis of laser targeting efficiency was calculated—both as the percent of the given state that received light delivery, and the percent of total recording time (over the first 6 h post-CFC) covered by light delivery (Supplementary Material, Fig. S5).

To assess the effects of rhythmic optogenetic stimulation of PV+ interneurons (Figs 4–6), *PV::ChR2* or *PV:GFP* transgenic mice were recorded from as described above. After CFC in the first hour after lights-on (ZT 0–1), both groups of mice underwent 6 h of SD by gentle handling in their home cage. Throughout the 6-h period SD, 473 nm laser light (CrystaLaser) was delivered to area CA1 bilaterally at 7 Hz (20 ms, square-wave pulses, power output estimated at 3–10 mW; Fig. 4A). As an additional control, 2 additional groups of *PV::ChR2* or *PV:GFP* mice underwent the same SD procedures, with light delivered to CA1 bilaterally throughout the 6-h period of SD at 18 Hz (10 ms, square-wave pulses; Fig. 5).

Following all optogenetic experiments, mice were perfused and brains were processed for histological assessment as described below. Optic fiber and electrode positions were validated prior to subsequent data analysis.

Single-Neuron Discrimination and Firing Analysis

Single neuron data were discriminated offline using standard principle component-based procedures (Offline Sorter; Plexon). Individual neurons were discriminated on the basis of spike waveform, relative spike amplitude on the 2 stereotrode recording wires, relative positioning of spike waveform clusters in 3D

principal component space, and neuronal subclass (i.e., fast-spiking [FS] interneurons or principal neurons). Spike cluster discrimination in principal component space was verified using MANOVA P values <0.05 and Davies–Bouldin (DB) indices ≥0.25, as previously described (Ognjanovski et al. 2017). Only those neurons that were reliably discriminated and continuously recorded throughout each experiment (i.e., those stably recorded across both 24-h baseline and 24-h post-CFC recording) were included in subsequent firing rate and coherence analyses. Post-CFC firing rate changes were calculated over 6-h windows for each neuron in NREM, REM, and wake as a percent change from baseline, as described previously (Ognjanovski et al. 2014).

Sleep/Wake Behavior and LFP Analyses

Intrahippocampal LFP and nuchal EMG signals were used to categorize each 10-s interval of recording as NREM, REM, or wake using custom software as previously described (Ognjanovski et al. 2014, 2017). The proportion of time spent in NREM, REM, and wake (and mean bout duration for each state) was calculated during the baseline and post-CFC recording periods for each mouse using standard conventions. Bouts were quantified as the interval between the beginning and end of a period in a single state; mean bout duration was used to determine whether optogenetic manipulations led to altered sleep architecture.

Raw LFP power was calculated between 0.5 and 300 Hz for each channel where stable single neuron data was obtained. Spectral power was quantified in 0.4 Hz bands at baseline, and following CFC; changes in spectral power from baseline were calculated as (power post CFC – power at baseline/power at baseline). For each recording channel, these values were summed across frequency bands for delta (0.5–4 Hz) and theta (4–12 Hz). Mean summed power changes were calculated (for all LFP channels recorded within the same hemisphere) for statistical comparisons of power changes between treatment groups. For correlation of power changes with learning, mean summed power changes were calculated for all LFP channels recorded in the same mouse. Ripples were detected using an algorithm that bandpass filtered LFPs to 150–250 Hz, set a voltage threshold ±2.0 standard deviations from baseline signal mean amplitude, and identified events where filtered LFP amplitude exceeded this threshold for 6 or more consecutive cycles. Using these criteria, baseline ripple frequency during NREM sleep was 0.1–0.5 Hz, consistent with previous reports (Csicsvari et al. 1999a; Girardeau et al. 2009; Stark et al. 2014). To compare ripple occurrence between baseline and post-CFC recording periods, ripples were detected across both recording intervals using the same (baseline) voltage threshold. Spectral power was calculated within detected ripple intervals at baseline and post-CFC, using the method described above.

Spectrograms of 0–12 Hz PSD activity were generated in MATLAB. PSD data for representative LFPs were calculated in 1-s windows, and PSDs were convolved over 30 s at 1 Hz. For Figures 1 and 4, PSDs were min–max normalized over the entirety of the selected temporal window (for comparison of different recordings); for Figure 3, raw spectral power is expressed as V^2/Hz, to illustrate absolute changes in LFP power with optogenetic inhibition.

Functional Connectivity and Functional Network Stability Analysis

Functional connectivity in CA1 was assessed using custom software as described previously (Ognjanovski et al. 2014, 2017). Briefly, pairwise function connectivity was quantified using spike trains $\{S_1, S_2, \ldots, S_n\}$ for n stably recorded CA1 neurons. The functional relationship FC_{ij} was calculated for each pair of neurons (e.g., i-th and j-th neurons) by first calculating the average temporal proximity of spike trains S_i and S_j. The average distance from spike train S_i to S_j is given by the average minimum distance (AMD) (Feldt et al. 2009). The AMD value was then compared with the expected sampling distance calculated from interspike intervals (ISIs) in S_j. Functional connectivity measures thus quantify the significance of mean temporal proximity of S_i to S_j after taking into account the spiking distributions of S_j, as previously described (Ognjanovski et al. 2017; Wu et al. 2018).

For each minute of recording time, relative pairwise connectivity across the network was quantified as a functional connectivity matrix (see Figs 6A and 7A). Matrices for each of the 1-min time windows were compared with one another in a pairwise fashion as previously described (Ognjanovski et al. 2017; Wu et al. 2018), to yield a similarity value between the 2 windows' connectivity patterns. A similarity value of 1 denotes no change in the network between timepoints, and a value of 0 indicates that the 2 networks are completely unrelated. A comparison of all existing windows for a given state and period of recording time yielded a functional similarity matrix (FSM; Fig. 6). To measure functional network stability (FuNS; Fig. 7), connectivity matrices in adjacent windows were compared across the entire recording—mean similarity values for a given segment of recording constituted the metric.

Immunohistochemistry

At the end of each recording, mice were deeply anesthetized with pentobarbital. All electrode sites were lesioned (2 mA, 3 s per wire), and mice were perfused with ice cold 0.1 M phosphate buffered saline (PBS), followed by 4% paraformaldehyde in PBS. Brains were removed, postfixed, and sectioned at 50 µm. Brain sections containing dorsal CA1 were immunostained with goat antiparvalbumin (1:1000; Abcam; ab11427) and were mounted using DAPI Fluoromount-G (Southern Biotech) to confirm transgene expression in PV+ interneurons.

To confirm Arch-mediated inhibition of PV+ interneurons, *PV::Arch* mice underwent single-trial CFC (a manipulation that induces high levels of cFos expression in PV+ interneurons) (Ognjanovski et al. 2017), and were immediately returned to their home cage, where 532 nm light was delivered to right hemisphere CA1. And 90 min later, each mouse was perfused as described above; brain sections were immunostained with rabbit anti-cFos (1:6250; Millipore; PC05). Quantification of cFos immunoreactivity in PV+ interneurons was conducted by a scorer blind to treatment conditions, following previously published methods (Ognjanovski et al. 2017). Briefly, for the 2 hemispheres in each brain slice, the number of CA1 neurons expressing GFP (i.e., those neurons with CRE-mediated transgene expression) was first counted. Laser-induced changes in PV+ interneuron activity were assessed by quantifying the percentage of GFP-expressing neurons which were also cFos immunopositive (# of cells cFos positive/# of GFP-positive cells). Comparisons were made between right (laser) and left (no-laser control) hemispheres in the same mouse. On the control hemisphere, cFos positive PV+ interneuron counts after CFC were similar to those in previous studies (Ognjanovski et al. 2017).

Software and Data Availability

All custom software and data supporting the findings of this study are available on request from the corresponding author.

Results

SD Disrupts Postlearning CA1 Network Coherent Firing and Oscillation Changes

To better understand the network dynamics associated with postlearning sleep, we first recorded CA1 network activity from C57BL/6J mice over a 24-h period before and after CFC (Fig. 1A; Supplementary Material, Fig. S1). Mice allowed *ad lib* sleep were compared with those sleep deprived over the first 6 h post-CFC (SD) (Fig. 1A). Consistent with previous data (Graves et al. 2003; Vecsey et al. 2009), SD mice showed significant deficits in CFM consolidation, assessed behaviorally as context-specific freezing 24 h after CFC (Fig. 1B). Overall LFP power in CA1 across both delta and theta frequencies was increased after CFC, consistent with previous findings (Ognjanovski et al. 2014, 2017) (Fig. 1C; Supplementary Material, Fig. S2B). While increases in delta power were enhanced across SD (consistent with increased activity in this frequency band seen across species during a prolonged period of enforced wake) (Aeschbach et al. 1997; Porrino et al. 2005; De Gennaro et al. 2007; Stephenson et al. 2015), post-CFC theta increases in CA1 were blunted by SD (Fig. 1D, Supplementary Material, Fig. S2). There was a trend for theta (but not delta) power changes in the 6 h following CFC to predict CFM consolidation in individual mice (although this did not reach statistical significance; Bonferroni-correct P-value = 0.07, R = 0.67, Spearman rank order). Delta- and theta-frequency coherence of CA1 neurons' firing was also increased for several hours after CFC in sleeping, but not SD, mice (Fig. 1E). Our prior findings suggest that learning-induced, coherent network oscillations during postlearning sleep may stabilize neuronal firing patterns across CA1 (Ognjanovski et al. 2014, 2017). Thus, we speculated that coherent firing during post-CFC sleep plays a causal role in promoting hippocampal memory storage.

NREM-Targeted Inhibition of CA1 PV+ Interneurons Disrupts Network Activity and CFM in a Manner Similar to SD

Because theta and delta activity are naturally enhanced in CA1 across all behavioral states following CFC (Fig. 1C; Supplementary Material, Fig. S2B), we first sought to determine whether state-specific changes in CA1 firing patterns were required for CFM consolidation. We have previously shown that long-term, state-independent inhibition of PV+ interneurons in CA1 can disrupt CFM consolidation (Ognjanovski et al. 2017). To manipulate network activity in a state-specific manner, we inhibited dorsal CA1 PV+ interneurons optogenetically during bouts of either NREM, REM, or wake, over the first 6 h following CFC. 532 nm laser light was targeted to CA1 bilaterally in mice expressing either GFP or archaerhodopsin in PV+ interneurons (*PV::GFP* or *PV::Arch*; Fig. 2A, Supplementary Material, Figs S3 and S4). Inhibition of PV+ interneuron activity during NREM, but not REM or wake, abolished CFM consolidation (Fig. 2C). NREM-targeted inhibition did not affect overall sleep architecture (which was similar across

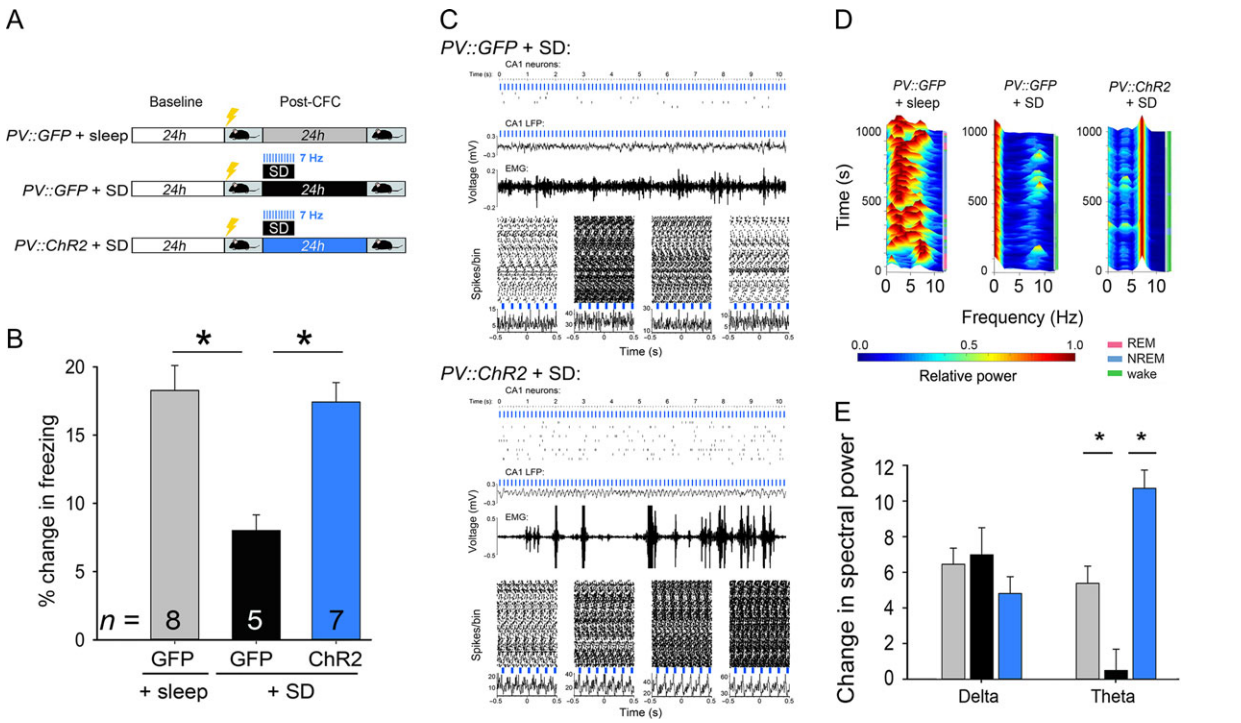

Figure 4. Rhythmic activation of PV+ interneurons rescues CFM consolidation and CA1 network activity rhythms disrupted by SD. (*A*) Experimental paradigm. *PV::GFP* mice either were allowed *ad lib* sleep after CFC, or received 6 h of post-CFC SD. *PV::ChR2* mice also received 6 h of SD. 473 nm light was delivered to CA1 bilaterally at 7 Hz, in 20 ms pulses, throughout SD procedures in both groups. (*B*) CFM was impaired following SD in *PV::GFP* mice. SD-induced CFM deficits were not seen in *PV::ChR2* mice with rhythmic optogenetic activation of PV+ interneurons. *$P < 0.05$, Holm–Sidak post hoc test. n indicates the number of mice per group. (*C*) Example traces of CA1 neurons' spike rasters, LFP activity, and EMG signals from representative *PV::GFP* and *PV::ChR2* mice, recorded during SD with 7 Hz light delivery. Peripulse rasters and histograms are shown for 4 representative neurons recorded simultaneously over a 10-min period from each mouse. (*D*) Min–max normalized CA1 LFP spectrograms are shown from the first 6 h post-CFC, for representative *PV::GFP* + sleep, *PV::GFP* + SD, and *PV::ChR2* + SD mice. (*E*) Over the first 6 h post-CFC, increases in CA1 delta power were similar across all groups while, theta power increases seen in freely sleeping *PV::GFP* mice were disrupted by SD. Theta increases were rescued by rhythmic optogenetic stimulation of PV+ interneurons. *$P < 0.005$, Holm–Sidak post hoc test; n = 12, 10, and 10 CA1 recordings for *PV::GFP* + sleep, *PV::GFP* + SD, and *PV::ChR2* + SD, respectively. All bar graphs indicate mean ± SEM values for each group.

treatment groups; Supplementary Material, Fig. S5A,B), but strongly altered CA1 network activity (Fig. 3). While sleep-associated theta and delta activity increased significantly after CFC in *PV::GFP* mice, NREM-targeted inhibition in *PV::Arch* mice significantly decreased delta and theta (relative to baseline NREM sleep; Fig. 3A,B). NREM-targeted PV+ interneuron inhibition also decreased LFP theta power during subsequent REM bouts in *PV::Arch* mice (Fig. 3B, bottom panel). Across animals, post-CFC increases in NREM delta and REM theta were predictive of successful CFM consolidation (Fig. 3C). NREM-targeted PV+ interneuron inhibition also suppressed post-CFC increases in the amplitude of SPWR oscillations in CA1 (Ognjanovski et al. 2017), and previously described post-CFC firing rate changes (Supplementary Material, Figs S2A and S6C) (Ognjanovski et al. 2014). Taken together, post-CFC changes in CA1 oscillations and neuronal firing were similar in direction and magnitude between mice with NREM-targeted PV+ interneuron inhibition and those with post-CFC SD. This suggests a similar network-level mechanism may underlie the disruption of CFM caused by either SD or NREM-targeted inhibition.

Disruption of CFM consolidation was specific to disruption of PV+ interneurons' activity during NREM sleep. Total optogenetic inhibition time for PV+ interneurons was greatest for mice with wake-targeted inhibition; in these mice, CFM consolidation was unaffected (Fig. 2; Supplementary Material, Fig. S5D).

Rhythmic Activation of CA1 PV+ Interneurons Rescues CFM From Disruption by SD

CA1 theta-frequency activity (across mouse strains and behavioral states) consistently predicts successful CFM consolidation, and experimental manipulations that disrupt this rhythm also impair memory storage (Boyce et al. 2016; Ognjanovski et al. 2017). We next tested whether theta-frequency CA1 activity patterns, present in the context of SD, could rescue CFM deficits. We generated a theta (7-Hz) oscillation optogenetically across a 6-h period of post-CFC SD, by rhythmically activating channelrhodopsin (ChR2)-expressing (Lin 2011; Zhao et al. 2011) PV+ interneurons in CA1. A 473 nm light was delivered in 20 ms pulses to CA1 bilaterally in *PV::ChR2* mice or *PV::GFP* control mice over the entire 6-h SD window (Fig. 4A, Supplementary Material, Figs S7, S8, and S9). CFM was compared between these 2 groups of SD mice (*PV::GFP* + SD and *PV::ChR2* + SD), and a third group with uninterrupted post-CFC sleep (*PV::GFP* + sleep). Rhythmic PV+ interneuron activation across SD restored CFM to levels seen in freely sleeping mice (Fig. 4B).

Consistent with prior findings (Amilhon et al. 2015; Ognjanovski et al. 2017) 7 Hz optogenetic stimulation of PV+ interneurons was sufficient to generate high-amplitude LFP oscillations and coherent firing among neighboring principal neurons (which fired in antiphase with light pulses, consistent with rhythmic inhibitory control of spike timing). We find that this is true even in the context of enforced, active wake during SD (Fig. 4C). In contrast, similar to what was seen in C57BL/6J mice (Fig. 1C,D), SD in GFP-expressing mice disrupted the naturally occurring post-CFC increases in CA1 theta activity seen in mice allowed *ad lib* sleep (Fig. 4D,E). In sleep-deprived ChR2-expressing mice, CA1 theta activity generated in CA1 by optogenetic stimulation was equal to or greater than that seen in freely sleeping mice after CFC. At the same time, theta-frequency stimulation did not alter the occurrence of SPWRs in CA1. The frequency of SPWR events was increased to the same level in the hours following CFC, regardless of behavioral state (*ad lib* sleep or SD), in *PV::GFP* + SD, *PV::ChR2* + SD, and *PV::GFP* + sleep groups (Supplementary Material, Fig. S8D). There was no consistent phase relationship between SPWRs and optogenetically induced theta oscillations.

To determine whether rescue of memory consolidation was related to the increased coherent firing induced by optogenetic stimulation, we next tested whether rhythmic stimulation at a frequency which does not induce the same degree of network coherence (18 Hz) (Ognjanovski et al. 2017) rescued CFM in a similar way. As shown in Figure 5, delivery of light pulses at 18 Hz, rather than 7 Hz, did not rescue CFM consolidation from SD-induced deficits in *PV::ChR2* + SD mice.

Rhythmic Activation of CA1 PV+ Interneurons Stabilizes CA1 Network Dynamics

In order to visualize how PV+ interneuron-driven oscillations change CA1 network communication in the hours following CFC, we generated a FSM (see Materials and Methods and Fig. 6A) (Ognjanovski et al. 2017) for each recording. The FSM quantifies the degree of similarity between a functional connectivity pattern (i.e., for a network of stably recorded neurons) at one time point versus all others across a recording. This quantification provides a dynamic view of neuronal networks over a timescale of hours. FSMs are shown for stably recorded CA1 neurons in representative mice, over the first 6 h of baseline recording and the first 6 h post-CFC (Fig. 6B). In freely sleeping mice, CFC led to a long-lasting period of more consistent repetition of specific network functional connectivity patterns;

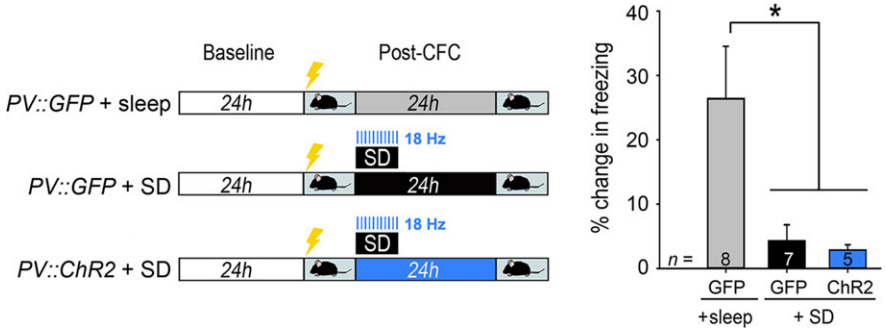

Figure 5. Optogenetic stimulation at 18 Hz does not rescue CFM from SD-induced deficits. In a second cohort of experimental mice, the behavioral paradigm was as described for Figure 3, but blue light was delivered to CA1 bilaterally at 18 Hz, a frequency which does not drive highly coherent firing in CA1 principal neurons (Ognjanovski et al. 2017). Deficits in CFM consolidation were seen in both *PV::GFP* + SD, and *PV::ChR2* + SD mice with 18 Hz light delivery to CA1. *$P < 0.05$, Holm–Sidak post hoc test. *PV::GFP* + SD versus *PV::ChR2* + SD, N.S. Bar graphs indicate mean ± SEM values for each group. *n* indicates the number of mice per group.

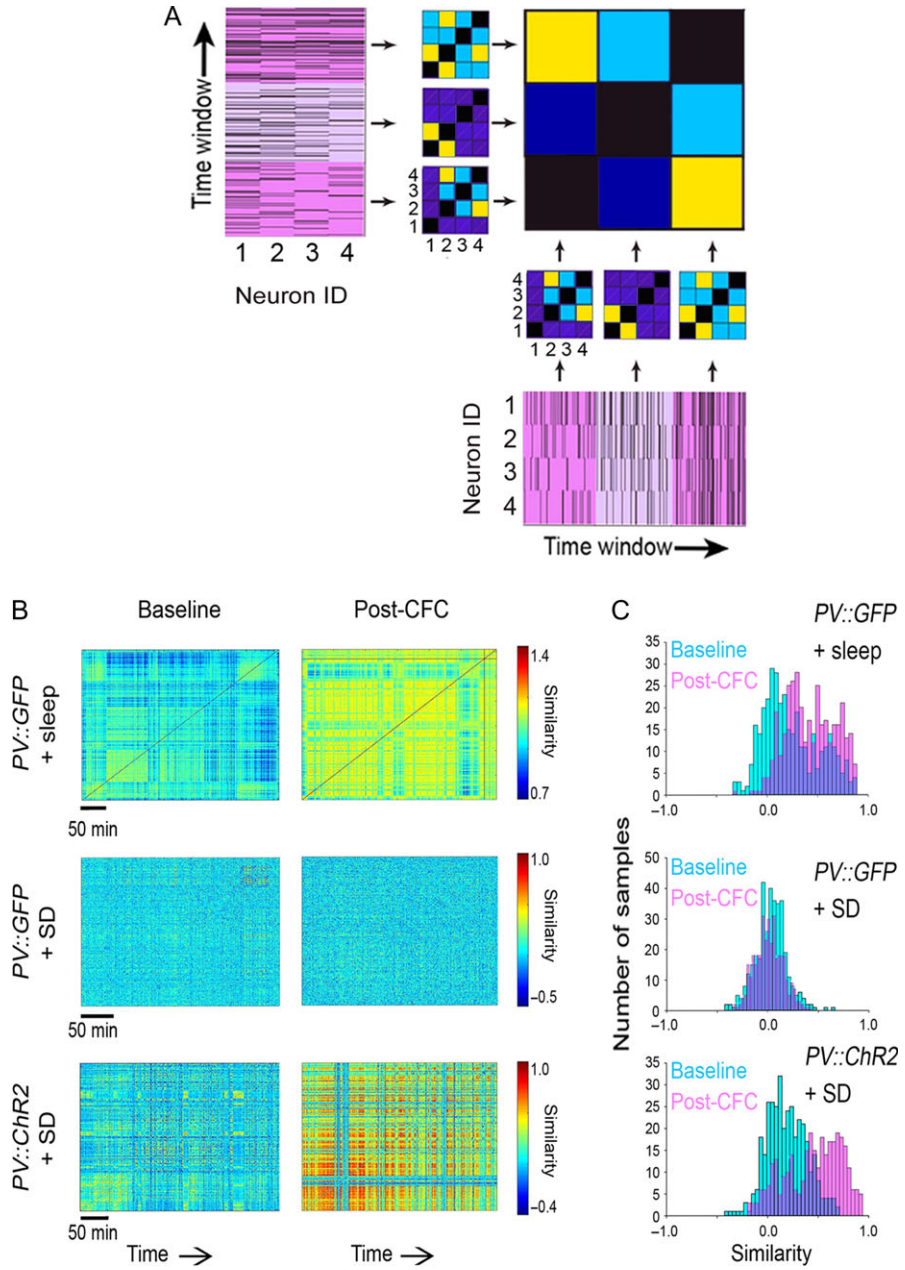

Figure 6. Rhythmic activation of PV+ interneurons coordinates CA1 ensembles. (*A*) Generation of a functional similarity matrix (FSM). Pairwise functional connectivity values are first calculated for every 1-min interval, based on spike trains of stably recorded neurons. From these values, a functional connectivity matrix is generated, which represents the pattern of functional connectivity at each time point. Pairs of neurons with stronger versus weaker functional connectivity are shown with warm and cool colors, respectively. The FSM displays the similarity of functional connectivity patterns for the same population of stably recorded neurons across recording time intervals. High and low similarity of connectivity patterns between timepoints is indicated by warm and cool colors, respectively. (*B*) CA1 network FSMs are shown for representative mice at baseline and over the first 6 h post-CFC. SD disrupted post-CFC enhancements in similarity of network communication patterns over time; these enhancements were rescued by rhythmic optogenetic stimulation of PV+ interneurons. Scale bars = 50 min of recording time. (*C*) Distributions of minute-to-minute similarity values (at baseline-blue, and following CFC-pink) are shown for the FSMs in (*B*).

this is quantified as a rightward shift in the distribution of similarity values after CFC (Fig. 6C). This change in network dynamics was prevented by post-CFC SD in *PV::GFP* mice, where similarity of functional connectivity patterns was unchanged after CFC. Optogenetically driven theta oscillations were sufficient to promote consistent reactivation of network activity patterns across a period of SD in *PV::ChR2* mice. Together, these findings show that PV+ interneuron-driven sleep oscillations promote long-term memory consolidation in the absence of sleep, possibly by promoting consistent reactivation of CA1 neuronal ensembles.

Stable CA1 Network Dynamics are a Consistent Predictor of Memory Formation

To further determine how the consistency of post-CFC CA1 network communication relates to memory formation, we quantified FuNS (see Materials and Methods and Fig. 7A) (Ognjanovski

et al. 2017) over baseline and post-CFC recording periods, across all treatment groups (Fig. 7). In freely sleeping mice, we observed an increase in the minute-to-minute FuNS, which lasted for many hours following CFC; this increase was disrupted by post-CFC SD (Fig. 7*B*). Post-CFC FuNS increases were also blocked in sleeping mice following NREM-targeted disruption of PV+ interneuron activity (Fig. 7*C*). Finally, similar to its effects on CFM consolidation, theta-frequency optogenetic stimulation of PV+ interneurons in CA1 was sufficient to rescue subsequent FuNS increases in SD mice, where normal post-CFC FuNS increases are typically lost (Fig. 7*D*). Across all treatments, increases in CA1 FuNS from baseline (e.g., in freely sleeping mice) tended to be higher in REM and NREM sleep than in wake (Fig. 7*B–D*). REM- and NREM-associated increases in FuNS, but not FuNS changes across periods of spontaneous wake, were predictive of successful CFM consolidation in individual mice (Fig. 7*E*). Thus, optogenetic manipulations of PV+ interneurons which disrupt or rescue CFM consolidation also disrupt or rescue, respectively, post-CFC stabilization of CA1 network functional connectivity patterns.

Discussion

While SD has been shown to affect multiple features of hippocampal function, including gene expression (Vecsey et al. 2012), protein synthesis (Tudor et al. 2016), and neuronal cytoskeletal dynamics (Havekes et al. 2016), we find that it also impacts both the rate and coherence of firing among CA1 neurons. Sleep in the first few hours following CFC (Prince et al. 2014) is known to be critical for consolidation of CFM. Importantly, pharmacological inhibition of CA1 network activity over the same time period similarly disrupts CFM (Daumas et al. 2005; Graves et al. 2003). We speculated that the oscillatory patterning of CA1 neuronal firing during post-CFC sleep might be critical for appropriate regulation of spike timing in the context of memory formation. In the present studies, the effects of bidirectional manipulations of CA1 oscillations on both CFM consolidation, and the associated changes in CA1 network communication patterns, suggest that this is indeed the case.

What Features of Sleep Physiology Support Memory?

Here we find that disruption of CA1 oscillatory dynamics (by optogenetically inhibiting PV+ interneurons during bouts of post-CFC NREM sleep) impairs CFM consolidation in a manner similar to SD. Critically, inhibition during NREM disrupts 3 key oscillations which have been implicated in sleep-dependent memory formation—delta, theta, and SPWRs. While SPWRs in particular have received extensive study as a potential driver of sequential replay events following spatial task performance (Puentes-Mestril and Aton 2017), the causal role of replay occurrence in memory consolidation remains unclear. Recently, we found that CFM consolidation is associated with long-lasting stabilization of CA1 network communication patterns (Ognjanovski et al. 2014). Most notably, in contrast to reports of sequential replay, this change to CA1 network dynamics can be measured over a relatively long timescale (i.e., 24 h or more), which reflects the period over which disruptions of either CA1 network activity, or sleep, can disrupt CFM consolidation (Graves et al. 2003; Misane et al. 2013; Prince et al. 2014). While the drivers of

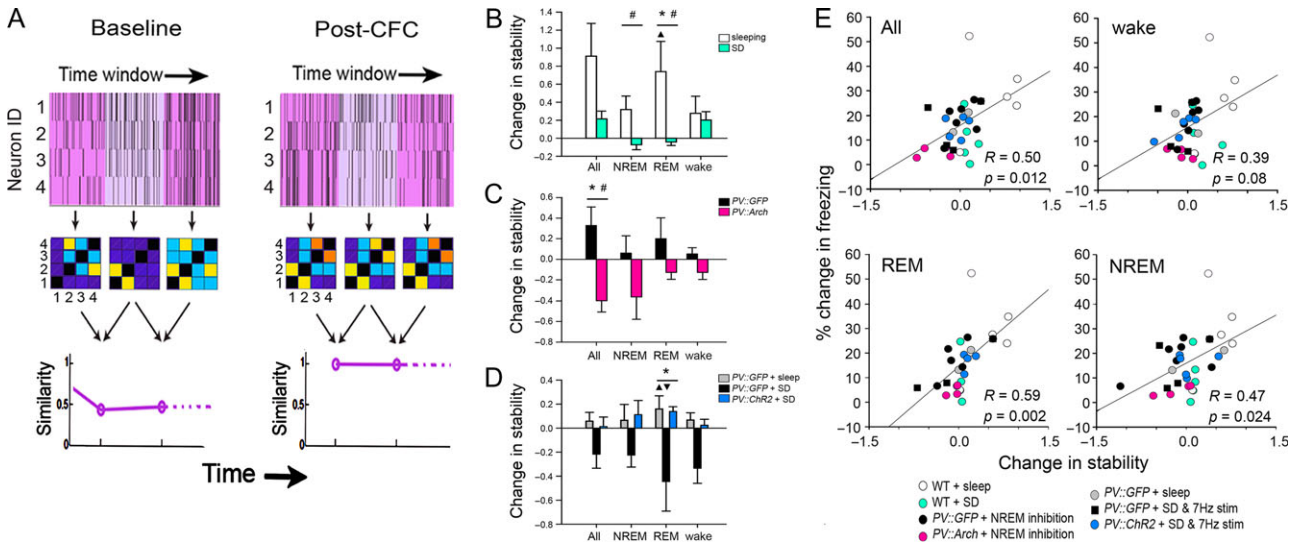

Figure 7. Increasing network stability following CFC is predictive of successful CFM consolidation. (*A*) Calculation of the functional network stability (FuNS) metric. Functional connectivity matrices are constructed for every 1-min interval of recording, based on spike rasters from stably recorded neurons. A comparison of matrices at adjacent time points yields a similarity value, which is plotted across the entirety of a recording period. FuNS is calculated for each animal as mean similarity value across a given recording period (baseline or post-CFC). (*B–D*) FuNS was assessed for populations of stably recorded CA1 neurons for all animals for all treatment groups from Figures 1–6. (*B*) In C57BL/6J mice, FuNS was increased (relative to baseline) after CFC in sleeping mice after the first 6 h of *ad lib* sleep, but was unchanged (relative to baseline) after post-CFC SD. *P < 0.05, Holm–Sidak post hoc test for sleep versus SD, ▲P < 0.01, Holm–Sidak post hoc test for baseline versus post-CFC; #P < 0.05, group × time interaction, 2-way RM ANOVA. Values are calculated from *n* = 50 (4–14/mouse) and 39 (5–13/mouse) stably recorded neurons for sleeping and SD groups, respectively. (*C*) NREM-targeted PV+ interneuron inhibition decreases overall FuNS for the first 12 h post-CFC. *P < 0.05, Holm–Sidak post hoc test for *PV::GFP* versus *PV::Arch*, #P < 0.05, group × time interaction, 2-way RM ANOVA. Values are calculated from *n* = 64 (8–16/mouse) and 44 (4–12/mouse) stably recorded neurons, respectively, from *PV::Arch* and *PV::GFP* mice. (*D*) Rhythmic optogenetic stimulation of PV+ interneurons during SD resulted in sustained increases in FuNS during subsequent REM sleep. *P < 0.05, Holm–Sidak post hoc test for *PV::GFP + sleep* versus *PV::GFP + SD*, and *PV::ChR2 + SD* versus *PV::GFP + SD*, ▲ and ▼P < 0.05, Holm–Sidak post hoc test for baseline versus post-CFC. All bar graphs indicate mean ± SEM values for each group. Values are calculated from *n* = 63 (3–12/mouse), 29 (4–9/mouse), and 48 (3–14/mouse) stably recorded neurons, respectively, from *PV::GFP* + sleep, *PV::GFP* + SD, and *PV::ChR2* + SD mice. (*E*) Increases in FuNS (over hours 0–12 post-CFC, vs. the same period in baseline) predicted successful CFM consolidation for individual animals across treatment groups. This effect was significant for periods of REM and NREM sleep, but not for periods of spontaneous wake. *R* and Bonferroni-corrected *P* values indicate results of Spearman rank order.

memory-associated network stabilization are still largely unknown, a likely mechanism to promote this process is rhythmic entrainment of CA1 neuronal firing by network oscillations associated with sleep. Such a mechanism would provide a timing cue that could regulate spike timing across the entire CA1 network. In support of this idea, we recently demonstrated (in anesthetized animals) that rhythmic optogenetic stimulation of CA1 PV+ interneurons at theta frequency (4–10 Hz) leads to both highly coherent firing and more stable functional communication patterns across the CA1 network. In contrast, stimulation outside this range (which fails to induce coherent firing) does not drive increases in FuNS (Ognjanovski et al. 2017). We also found that disruption of naturally occurring CA1 network oscillations (by pharmacogenetically inhibiting PV+ interneurons) following CFC leads to disruption of learning-induced FuNS increases (Ognjanovski et al. 2017).

In order to test the relationships between specific sleep-associated network oscillations, FuNS, and memory formation, we attempted to rescue CFM consolidation in sleep-deprived mice by generating coherent rhythms in CA1. Here, we found that stimulation of PV+ interneurons CA1 at a frequency normally augmented during post-CFC sleep (7 Hz) across a period of SD promoted CFM consolidation. There was no rescue by stimulation at 18 Hz—a frequency that is not normally enhanced during post-CFC sleep, and which we have previously shown does not drive highly coherent firing or increases in FuNS among CA1 neurons (Ognjanovski et al. 2017). Optogenetically driven 7-Hz rhythms also promoted the consistent reactivation of CA1 network communication patterns in the hours following CFC. Surprisingly, this manipulation had no effect on the occurrence of SPWRs, suggesting that lower-frequency oscillations alone may be sufficient both for stable ensemble activity patterning after CFC, and for memory storage. Taken together, these data indicate that network oscillations (which are normally augmented in postlearning sleep) promote consistent patterning of activity within CA1 ensembles, which in turn supports long-term memory storage.

Our finding that disruption of PV+ interneuron activity during post-CFC NREM bouts, but not REM bouts, impairs CFM might seem at odds with the recent report that inhibition of GABAergic medial septal input to the hippocampus during REM, but not NREM, impairs consolidation of object-place recognition memory (Boyce et al. 2016). Critically, this REM-targeted manipulation disrupts theta-frequency activity in CA1, in a manner similar to PV+ interneuron inhibition within CA1 (Boyce et al. 2016; Ognjanovski et al. 2017). We cannot conclude that CA1 activity during REM is unimportant, or unnecessary, for CFM consolidation, because 1) our NREM-targeted manipulation also disrupts REM theta (Fig. 3) and 2) across treatment groups, REM-associated FuNS increases predict successful memory storage (Fig. 7). However, targeting inhibition specifically to REM bouts does not similarly disrupt fear memory. This suggests that, in the absence of coherent NREM oscillations, REM-associated CA1 activity patterns may be insufficient for CFM consolidation.

What Drives Post-CFC Changes in the CA1 Network?

Two critical questions related to our present findings remain unanswered. The first is: what gives rise to the naturally occurring increase in CA1 network oscillations during post-CFC sleep? Recent studies have shown that CFC leads to activity-dependent plastic changes in CA3 and CA1 PV+ interneurons (Donato et al. 2014), and our own data suggest that CA1 PV+ interneurons remain highly active in the hours following CFC (based on high levels of cFos expression; Supplementary Material, Fig. S3) (Ognjanovski et al. 2017). Thus, one possibility is that post-CFC changes in hippocampal oscillations which normally regulated by PV+ interneurons are brought about simply by changes to PV+ circuitry. Another possibility is that these changes could be mediated by plasticity of septal (Berger and Thompson 1978), CA3 (Choi et al. 2018), or cortical (Carretero-Guillen et al. 2015) inputs to CA1 (all of which have been reported following learning).

A second, related question is, why are learning-associated changes in network activity disrupted by post-CFC SD? One possibility is that the cellular mechanisms required for the plastic changes described above rely on postlearning sleep. Sleep and SD differentially affect a number of cellular pathways involved in regulating plasticity in the hippocampus, including transcription of genes involved in synaptic function (Vecsey et al. 2012; Delorme et al. 2018) and protein translation (Tudor et al. 2016). These sleep-dependent biosynthetic events can vary as a function of prior learning (Ribeiro et al. 1999; Ulloor and Datta 2005; Calais et al. 2015), and may lead to structural changes in hippocampal neurons (Havekes et al. 2016). Another possible explanation is that sleep loss causes changes in network excitability that are incompatible with coherent network oscillations. Available data suggest that conditioning induces changes in neuronal excitability and firing rate in CA1 (McKay et al. 2009; Ognjanovski et al. 2014), and that SD can interfere with these processes (McDermott et al. 2003, 2006) (Supplementary Material, Fig. S2A). Both experimental and computational modeling data suggest that neuronal resonance with subthreshold membrane oscillations (such as those occurring during sleep) varies as a function of network plasticity and intrinsic excitability (Narayanan and Johnston 2007; Roach et al. 2018). A third possibility is that waking experience during SD simply interferes with these network activity patterns.

The Significance of Network Oscillations

Based on our present findings, and previous recordings of CA1 during CFM consolidation, the most consistent correlate of sleep-associated network oscillations is stable patterning of firing in CA1 ensembles (Ognjanovski et al. 2014, 2017). This increase in stable patterning (i.e., FuNS), over a period of hours, would provide an optimal condition for spike timing-dependent plasticity in the CA1 network. Changes in synaptic strength resulting from this process would allow de novo information storage in the CA1 network in the hours following learning. Our present finding that CA1 oscillatory dynamics alone, in the absence of sleep, is sufficient for memory storage reinforces the idea that oscillation-induced stabilization of firing patterns is an essential component of memory consolidation. Recent findings have proposed "replay"—sequential reactivation of neurons activated sequentially during a learning event—as a mechanism for consolidation. Replay, like increases observed in FuNS after learning, is also associated with network oscillations (Destexhe et al. 2007; Molle and Born 2011; Sadowski et al. 2011). Moreover, recent computational work from our lab suggests that coherent network oscillations are sufficient to generate both replay and FuNS increases, from the same network, following a learning event (Roach et al. 2018). One possibility, supported by computational data, is that sequential replay reflects a very specific form of FuNS increase—in which firing in the network is so stable that precisely timed sequences of firing among neurons can be reliably evoked, over and over (Roach et al. 2018; Wu et al. 2018). In this case, one

would expect that FuNS changes might be easier to detect in scenarios where sequential patterns of firing are not reported, such as after CFC.

(Vecsey et al. 2009; Aton et al. 2009a; Seibt et al. 2012; Dumoulin et al. 2015; Havekes et al. 2016; Tudor et al. 2016) Recent findings have shown that coherent rhythms of activity between brain areas (e.g., between hippocampus and cortex) are associated with memory storage across a period of sleep (Rothschild et al. 2017; Totty et al. 2017; Xia et al. 2017). An unanswered question is how these oscillations are coordinated between thalamocortical circuits and the hippocampus. One possibility is that hippocampal oscillations enhanced during sleep by prior learning (or in this case, oscillations that are optogenetically driven during SD) coordinate activity patterns in other brain areas. For example, Xia et al. (2017) recently demonstrated that coherence of hippocampal ripples with thalamocortical spindles is enhanced after CFC, and that pharmacogenetic inhibition of PV+ interneurons disrupts this coherence. Latchoumane et al. (2017) recently demonstrated that optogenetic inhibition or stimulation of PV+ thalamic reticular nucleus (TRN) neurons, which (respectively) disrupt or enhance synchrony between thalamocortical spindles, cortical slow oscillations, and hippocampal ripples, disrupt or enhance CFM consolidation. While TRN activity manipulations also have well-documented effects on sleep and arousal (Kim et al. 2012; Lewis et al. 2015), these findings nonetheless suggest that appropriate timing between thalamocortical and hippocampal oscillations may promote information storage in the context of memory consolidation. One technical limitation of our present study is that CA1 activity was recorded in isolation; no cortical recordings were made simultaneously to similarly assess coherence of hippocampal activity with thalamocortical oscillations (as others have done) (Staresina et al. 2015; Xia et al. 2017). Thus it remains to be determined how activity patterns in other brain areas are affected by theta rhythms generated in CA1.

A critical unanswered question is what intracellular signaling pathways, critical for memory consolidation, could be dysregulated during SD, and rescued by optogenetically driven network rhythms. Recent studies have shown that signaling pathways involved in protein synthesis (Tudor et al. 2016), actin cytoskeleton remodeling (Havekes et al. 2016), and protein phosphorylation (Vecsey et al. 2009) are all critical for CFM consolidation and dysregulated by SD. The same signaling pathways are also essential mediators of sleep-dependent plasticity elsewhere in the brain (e.g., in the visual system) (Aton et al. 2009a; Seibt et al. 2012; Dumoulin et al. 2015). Critically, these pathways are all activated in the context of activity-dependent synaptic remodeling (Puentes-Mestril and Aton 2017), and thus likely targets of optogenetic manipulations which regulate spike timing across the CA1 network. Future studies will be needed to determine how the manipulations of network activity described here impinge on signaling mechanisms involved in synaptic plasticity and other cellular functions essential for memory consolidation.

Conclusion

Many forms of memory consolidation appear to rely on post-learning sleep, both in animal models (Graves et al. 2003; Vecsey et al. 2009; Aton et al. 2009b; Vorster and Born 2015; Puentes-Mestril and Aton 2017) and in human subjects (Huber et al. 2004; Nishida and Walker 2007; Mednick et al. 2013). However, the mechanistic basis for sleep-dependent memory storage has remained elusive. Here we provide evidence that oscillatory dynamics that are naturally augmented in the hippocampus during sleep are both necessary (as we have shown previously (Ognjanovski et al. 2017)), and sufficient (in the absence of sleep, as we show here) for long-lasting memory storage. Our data indicate that these effects are likely related to long-timescale (i.e., hours) stabilization of communication patterns between neurons as a function of oscillatory dynamics in the network. Taken together, our findings suggest a neural network-level mechanism which can overcome cognitive deficits normally induced by sleep disruption.

Supplementary Material

Supplementary material is available at *Cerebral Cortex* online.

Funding

Young Investigator Award from the Brain and Behavior Research Foundation, an Alfred P. Sloan Foundation Fellowship, a Catalyst Grant from the Michigan Institute for Computational Discovery and Engineering, and the NIH (DP2MH104119 and R01EB018297).

Notes

The authors thank Drs Richard Hume and Monica Dus (Department of Molecular, Cellular, and Developmental Biology, University of Michigan) for helpful commentary on these studies. We are very grateful to Sha Jiang for expert technical assistance with this work, and Igor Belopolsky (Information Technology Advocacy and Research Support, College of Literature, Science and Arts, University of Michigan) for programming assistance. Lastly, the authors would like to thank members of the Zochowski lab for valuable input during the development of software for functional connectivity and network stability analysis. *Conflict of Interest*: The authors declare no conflicts of interest.

References

Aeschbach D, Matthews JR, Postolache TT, Jackson MA, Giesen HA, Wehr TA. 1997. Dynamics of the human EEG during prolonged wakefulness: evidence for frequency-specific circadian and homeostatic influences. Neurosci Lett. 239: 121–124.

Amilhon B, Huh CY, Manseau F, Ducharme G, Nichol H, Adamantidis A, Williams S. 2015. Parvalbumin interneurons of hippocampus tune population activity at theta frequency. Neuron. 86:1277–1289.

Aton SJ. 2013. Set and setting: how behavioral state regulates sensory function and plasticity. Neurobiol Learn Mem. 106: 1–10.

Aton SJ, Seibt J, Dumoulin M, Jha SK, Steinmetz N, Coleman T, Naidoo N, Frank MG. 2009a. Mechanisms of sleep-dependent consolidation of cortical plasticity. Neuron. 61: 454–466.

Aton SJ, Seibt J, Frank MG. 2009b. Sleep and memory. In: Encyclopedia of life science. Chichester: John Wiley and Sons, Ltd. http://www.els.net. doi: 10.1002/9780470015902.a0021395.pub2.

Aton SJ, Suresh A, Broussard C, Frank MG. 2014. Sleep promotes cortical response potentiation following visual experience. Sleep. 37:1163–1170.

Berger TW, Thompson RF. 1978. Neuronal plasticity in the limbic system during classical conditioning of the rabbit nictitating membrane response. II: Septum and mammillary bodies. Brain Res. 156:293–314.

Boyce R, Glasgow SD, Williams S, Adamantidis A. 2016. Causal evidence for the role of REM sleep theta rhythm in contextual memory consolidation. Science. 352:812–816.

Calais JB, Ojopi EB, Morya E, Sameshima K, Ribeiro S. 2015. Experience-dependent upregulation of multiple plasticity factors in the hippocampus during early REM sleep. Neurobiol Learn Mem. 122:19–27.

Carr MF, Karlsson MP, Frank LM. 2012. Transient slow gamma synchrony underlies hippocampal memory replay. Neuron. 75:700–713.

Carretero-Guillen A, Pacheco-Calderon R, Delgado-Garcia JM, Gruart A. 2015. Involvement of hippocampal inputs and intrinsic circuit in the acquisition of context and cues during classical conditioning in behaving rabbits. Cereb Cortex. 25: 1278–1289.

Choi J.h., Sim SE, Kim JI, Choi DI, Oh J, Ye S, Lee J, Kim T, Ko HG, Lim CS, et al. 2018. Interregional synaptic maps among engram cells underlie memory formation. Science. 360: 430–435.

Crunelli V, Lorincz ML, Connelly WM, David F, Hughes SW, Lambert RC, Leresche N, Errington AC. 2018. Dual function of thalamic low-vigilance state oscillations: rhythm-regulation and plasticity. Nat Rev Neurosci. 19:107–118.

Csicsvari J, Hirase H, Czurko A, Mamiya A, Buzsaki G. 1999a. Fast network oscillations in the hippocampal CA1 region of the behaving rat. J Neurosci. 19:RC20.

Csicsvari J, Hirase H, Czurko A, Mamiya A, Buzsaki G. 1999b. Oscillatory coupling of hippocampal pyramidal cells and interneurons in the behaving rat. J Neurosci. 19:274–287.

Daumas S, Halley H, Frances B, Lassalle JM. 2005. Encoding, consolidation, and retrieval of contextual memory: differential involvement of dorsal CA3 and CA1 hippocampal subregions. Learn Mem. 12:375–382.

De Gennaro L, Marzano C, Veniero D, Moroni F, Fratello F, Curcio G, Ferrara M, Ferlazzo F, Novelli L, Concetta Pellicciari M, et al. 2007. Neurophysiological correlates of sleepiness: a combined TMS and EEG study. Neuroimage. 36:1277–1287.

Delorme J, Kodoth V, Aton SJ. 2018. Sleep loss disrupts arc expression in dentate gyrus neurons. Neurobiol Learn Mem. Epub ahead of print.

Destexhe A, Hughes SW, Rudolph M, Crunelli V. 2007. Are corticothalamic 'up' states fragments of wakefulness? Trends Neurosci. 30(7):334–342. In Press, Corrected Proof.

Diekelmann S, Born J. 2010. The memory function of sleep. Nat Rev Neurosci. 11:114–126.

Donato F, Belluco S, Caroni P. 2014. Parvalbumin-expressing basket-cell network plasticity induced by experience regulates adult learning. Nature. 504:272–276.

Dragoi G, Buzsaki G. 2006. Temporal encoding of place sequences by hippocampal cell assemblies. Neuron. 50: 145–157.

Dumoulin MC, Aton SJ, Watson AJ, Renouard L, Coleman T, Frank MG. 2015. Extracellular signal-regulated kinase (ERK) activity during sleep consolidates cortical plasticity in vivo. Cereb Cortex. 25:507–515.

Dupret D, O'Neill J, Pleydell-Bouverie B, Csicsvari J. 2010. The reorganization and reactivation of hippocampal maps predict spatial memory performance. Nat Neurosci. 13: 995–1002.

Durkin JM, Suresh A, Colbath J, Broussard C, Wu J, Zochowski M, Aton SJ. 2017. Thalamocortical oscillations in NREM sleep play an essential, instructive role in visual system plasticity. Proc Natl Acad Sci USA. 114:10485–10490.

Feldt S, Waddell J, Hetrick VL, Berke JD, Żochowski M. 2009. Functional clustering algorithm for the analysis of dynamic network data. Phys Rev E. 79:056104.

Girardeau G, Benchenane K, Wiener SI, Buzsaki G, Zugaro MB. 2009. Selective suppression of hippocampal ripples impairs spatial memory. Nat Neurosci. 12:1222–1223.

Goshen I, Brodsky M, Prakash R, Wallace J, Gradinaru V, Ramakrishnan C, Deisseroth K. 2011. Dynamics of retrieval strategies for remote memories. Cell. 147:678–689.

Graves LA, Heller EA, Pack AI, Abel T. 2003. Sleep deprivation selectively impairs memory consolidation for contextual fear conditioning. Learn Mem. 10:168–176.

Havekes R, Park AJ, Tudor JC, Luczak VG, Hansen RT, Ferri SL, Bruinenberg VM, Poplawski SG, Day JP, Aton SJ, et al. 2016. Sleep deprivation causes memory deficits by negatively impacting neuronal connectivity in hippocampal area CA1. eLife. 5;pii: e13424. doi: 10.7554/eLife.13424.

Huber R, Ghilardi MF, Massimini M, Tononi G. 2004. Local sleep and learning. Nature. 430:78–81.

Inostroza M, Born J. 2013. Sleep for preserving and transforming episodic memory. Annu Rev Neurosci. 36:79–102.

Itskov V, Pastalkova E, Mizuseki K, Buzsaki G, Harris KD. 2008. Theta-mediated dynamics of spatial information in hippocampus. J Neurosci. 28:5959–5964.

Kim A, Latchoumane C, Lee SH, Kim GB, Cheong E, Augustine GJ, Shin HS. 2012. Optogenetically induced sleep spindle rhythms alter sleep architectures in mice. Proc Natl Acad Sci USA. 109:20673–20678.

Knowlton B, McGowan M, Olton DS. 1985. Hippocampal stimulation disrupts spatial working memory even 8 h after acquisition. Behav Neural Biol. 44:325–337.

Kudrimoti HS, Barnes CA, McNaughton BL. 1999. Reactivation of hippocampal cell assemblies: effects of behavioral state, experience and EEG dynamics. J Neurosci. 19:4090–4101.

Latchoumane CV, Ngo HV, Born J, Shin HS. 2017. Thalamic spindles promote memory formation during sleep through triple phase-locking of cortical, thalamic, and hippocampal rhythms. Neuron. 95:424–435.

Lewis LD, Voigts J, Flores FJ, Schmitt LI, Wilson MA, Halassa MM, Brown EN. 2015. Thalamic reticular nucleus induces fast and local modulation of arousal state. eLife. 4:e08760.

Lin JY. 2011. A user's guide to channelrhodopsin variants: features, limitations and future developments. Exp Physiol. 96:19–25.

McDermott CM, Hardy MN, Bazan NG, Magee JC. 2006. Sleep deprivation-induced alterations in excitatory synaptic transmission in the CA1 region of the rat hippocampus. J Physiol. 570:353–365.

McDermott CM, LaHoste GJ, Chen C, Musto A, Bazan NG, Magee JC. 2003. Sleep deprivation causes behavioral, synaptic, and membrane excitability alterations in hippocampal neurons. J Neurosci. 23:9687–9695.

McKay BM, Matthews EA, Oliveira FA, Disterhoft JF. 2009. Intrinsic neuronal excitability is reversibly altered by a single experience in fear conditioning. J Neurophysiol. 102: 2763–2770.

Mednick SC, McDevitt EA, Walsh JK, Wamsley E, Paulus M, Kanady JC, Drummond SPA. 2013. The critical role of sleep spindles in hippocampal-dependent memory: a pharmacology study. J Neurosci. 33:4494–4504.

Misane I, Kruis A, Pieneman AW, Ogren SO, Stiedel O. 2013. GABA(A) receptor activation in the CA1 area of the dorsal hippocampus impairs consolidation of conditioned contextual fear in C57BL/6J mice. Behav Brain Res. 238:160–169.

Molle M, Born J. 2011. Slow oscillations orchestrating fast oscillations and memory consolidation. Prog Brain Res. 193:93–110.

Narayanan R, Johnston D. 2007. Long-term potentiation in rat hippocampal neurons is accompanied by spatially widespread changes in intrinsic oscillatory dynamics and excitability. Neuron. 56:1061–1075.

Ngo HV, Martinez T, Born J, Molle M. 2013. Auditory closed-loop stimulation of the sleep slow oscillation enhances memory. Neuron. 78:545–553.

Nishida M, Walker MP. 2007. Daytime naps, motor memory consolidation and regionally specific sleep spindles. PLoS One. 2:e341.

Ognjanovski N, Maruyama D, Lashner N, Zochowski M, Aton SJ. 2014. CA1 hippocampal network activity changes during sleep-dependent memory consolidation. Front Syst Neurosci. 8:61.

Ognjanovski N, Schaeffer S, Mofakham S, Wu J, Maruyama D, Zochowski M, Aton SJ. 2017. Parvalbumin-expressing interneurons coordinate hippocampal network dynamics required for memory consolidation. Nature Commun. 8: 16120.

Ong JL, Lo JC, Chee NI, Santostasi G, Paller KA, Zee PC, Chee MW. 2016. Effects of phase-locked acoustic stimulation during a nap on EEG spectra and declarative memory consolidation. Sleep Med. 20:88–97.

Porrino L, Daunais J, Rogers G, Hampson R, Deadwyler S. 2005. Facilitation of task performance and removal of the effects of sleep deprivation by an ampakine (CX717) in nonhuman primates. PLoS Biol. 3:e299.

Prince TM, Wimmer M, Choi J, Havekes R, Aton S, Abel T. 2014. Sleep deprivation during a specific 3-hour time window post-training impairs hippocampal synaptic plasticity and memory. Neurobiol Learn Mem. 109:122–130.

Puentes-Mestril C, Aton SJ. 2017. Linking network activity to synaptic plasticity during sleep: hypotheses and recent data. Front Neural Circuits. 11:61. doi:10.3389/fncir.2017.00061.

Ribeiro S, Gervasoni D, Soares ES, Zhou Y, Lin SC, Pantoja J, Lavine M, Nicolelis MA. 2004. Long-lasting novelty-induced neuronal reverberation during slow-wave sleep in multiple forebrain areas. PLoS Biol. 2:E24.

Ribeiro S, Goyal V, Mello CV, Pavlides C. 1999. Brain gene expression during REM sleep depends on prior waking experience. Learn Mem. 6:500–508.

Roach JP, Pidde O, Katz E, Wu J, Ognjanovski N, Aton SJ, Zochowski M. 2018. Resonance with subthreshold oscillatory drive organizes activity and optimizes learning in neural networks. Proc Natl Acad Sci USA. 114:10485–10490.

Ross RS, Eichenbaum H. 2006. Dynamics of hippocampal and cortical activation during consolidation of a nonspatial memory. J Neurosci. 26:4852–4859.

Rothschild G, Eban E, Frank LM. 2017. A cortical–hippocampal–cortical loop of information processing during memory consolidation. Nat Neurosci. 20:251–259.

Sadowski JH, Jones MW, Mellor JR. 2011. Ripples make waves: binding structured activity and plasticity in hippocampal networks. Neural Plast. 2011:960389.

Seibt J, Dumoulin M, Aton SJ, Coleman T, Watson A, Naidoo N, Frank MG. 2012. Protein synthesis during sleep consolidates cortical plasticity in vivo. Curr Biol. 22:676–682.

Staresina BP, Ole Bergmann T, Bonnefond M, van der Meij R, Jensen O, Deuker L, Elger CE, Axmacher N, Fell J. 2015. Hierarchical nesting of slow oscillations, spindles, and ripples in the human hippocampus during sleep. Nat Neurosci. 18:1679–1686.

Stark E, Roux L, Eichler R, Senzai Y, Royer S, Buzsaki G. 2014. Pyramidal cell-interneuron interactions underlie hippocampal ripple oscillations. Neuron. 83:467–480.

Stephenson R, Caron AM, Famina S. 2015. Behavioral sleep-wake homeostasis and EEG delta power are decoupled by chronic sleep restriction in the rat. Sleep. 38:685–697.

Tononi G, Cirelli C. 2014. Sleep and the price of plasticity: from synaptic and cellular homeostasis to memory consolidation and integration. Neuron. 81:12–34.

Totty MS, Chesney LA, Geist PA, Datta S. 2017. Sleep-dependent oscillatory synchronization: a role in fear memory consolidation. Front Neural Circuits. 11:49.

Tudor JC, Davis EJ, Peixoto L, Wimmer ME, van Tilborg E, Park AJ, Poplawski SG, Chung CW, Havekes R, Huang J, et al. 2016. Sleep deprivation impairs memory by attenuating mTORC1-dependent protein synthesis. Sci Signal. 9:ra41.

Ulloor J, Datta S. 2005. Spatio-temporal activation of cyclic AMP response element-binding protein, activity-regulated cytoskeletal-associated protein and brain-derived nerve growth factor: a mechanism for pontine-wave generator activation-dependent two-way active-avoidance memory processing in the rat. J Neurochem. 95:418–428.

Vecsey CG, Baillie GS, Jaganath D, Havekes R, Daniels A, Wimmer M, Huang T, Brown KM, Li XY, Descalzi G, et al. 2009. Sleep deprivation impairs cAMP signalling in the hippocampus. Nature. 461:1122–1125.

Vecsey CG, Peixoto L, Choi JH, Wimmer M, Jaganath D, Hernandez PJ, Blackwell J, Meda K, Park AJ, Hannenhalli S, et al. 2012. Genomic analysis of sleep deprivation reveals translational regulation in the hippocampus. Physiol Genomics. 44(20):981–991. Epub ahead of print.

Vorster AP, Born J. 2015. Sleep and memory in mammals, birds, and invertebrates. Neurosci Biobehav Rev. 50:103–119.

Westerberg CE, Florczak SM, Weintraub S, Mesulam MM, Marshall L, Zee PC, Paller KA. 2015. Memory improvement via slow-oscillatory stimulation during sleep in older adults. Neurobiol Aging. 36:2577–2586.

Wierzynski C, Lubenov E, Gu M, Siapas A. 2009. State-dependent spike-timing relationships between hippocampal and prefrontal circuits during sleep. Neuron. 61:587–596.

Wu J, Skilling Q, Maruyama D, Li C, Ognjanovski N, Aton SJ, Zochowski M. 2018. Functional network stability and average minimal distance—a framework to rapidly assess dynamics of functional network representations. J Neurosci Methods. 296:69–83.

Xia F, Richards BA, Tran MM, Josselyn SA, Takehara-Nishiuchi K, Frankland PW. 2017. Parvalbumin-positive interneurons mediate neocortical-hippocampal interactions that are necessary for memory consolidation. eLife. 6:e27868.

Zhao S, Ting JT, Atallah HE, Qiu L, Tan J, Gloss B, Augusting GJ, Deisseroth K, Luo M, Graybiel AM, et al. 2011. Cell type–specific channelrhodopsin-2 transgenic mice for optogenetic dissection of neural circuitry function. Nat Methods. 8: 745–752.